Available online at www.sciencedirect.com
ScienceDirect
Journal of Power Sources 176 (2008) 460–467
JOURNAL OF POWER SOURCES
www.elsevier.com/locate/jpowsour

Compact direct methanol fuel cells for portable application

U.A. Icardi, S. Specchia*, G.J.R. Fontana, G. Saracco, V. Specchia

Materials Science and Chemical Engineering Dept., Politecnico di Torino, Corso Duca degli Abruzzi 24, 10129 Torino, Italy

Available online 25 August 2007

Abstract

Consumers' demand for portable audio/video/ICT products has driven the development of advanced power technologies in recent years. Fuel cells are a clean technology with low emissions levels, suitable for operation with renewable fuels and capable, in a next future, of replacing conventional power systems meeting the targets of the Kyoto Protocol for a society based on sustainable energy systems. Within such a perspective, the objective of the European project MOREPOWER (compact direct methanol fuel cells for portable applications) is the development of a low-cost, low temperature, portable direct methanol fuel cell (DMFC; nominal power 250 W) with compact construction and modular design for the potential market area of weather stations, medical devices, signal units, gas sensors and security cameras. This investigation is focused on a conceptual study of the DMFC system carried out in the Matlab/Simulink® platform: the proposed scheme arrangements lead to a simple equipment architecture and a efficient process.

Keywords: Direct methanol fuel cell; Portable devices; Modelling; Compactness

1. Introduction

Fuel cells (FCs) are ideal devices to generate electricity from either fossil or renewable fuels: they are a clean and efficient energy supply system, with low emissions levels, capable, in a next future, to replace conventional power systems thereby meeting the targets of the Kyoto Protocol on the reduction of EU green house gases by 8% in 2008 and even beyond the Kyoto deadline of 2010 [1]. The introduction of portable FCs in the market will bring considerable advance in this power-supply sector [2]. Direct methanol fuel cells (DMFCs) are attractive for several applications in view of their lower weight and volume compared with indirect FCs. DMFCs are increasingly being developed to replace or support batteries, mainly for the high energy density of methanol (MeOH) [3]. DMFCs are promising candidates as portable power sources because they do not require any fuel processing and operate at low temperatures (30–60 °C) [4]. The elimination of the fuel processor results in a simpler design and operation, higher reliability, lower weight, volume and capital/operating costs. Other potential advantages, despite the lower performance obtainable compared to PEMFCs, due to both MeOH crossover and slow kinetics of the redox reaction [5], are (i) the use of a liquid fuel and (ii) the absence of complex humidification and thermal management systems as required for PEMFCs [2,6]. However, the current component developments carried out worldwide is leading to significant performance improvements. For instance, DMFC systems with a power density up to 200 mW cm^{-2} at 120 °C and 120 mW cm^{-2} at 80 °C were recently developed by using Pt catalyst and pressurized air at the cathode side [7]. In terms of power density, the performance of a DMFC is still significantly lower (about 30% efficiency at 80 °C) compared to a PEMFCs [8]. Moreover, more and more attention is being devoted to improve the overall performance of DMFCs thanks to the development of novel and low-cost proton exchange membranes with reduced fuel crossover through the electrolyte compared to that of currently available materials, e.g. Nafion® [9–12]. New electro-catalysts are also under development to enhance the low temperature MeOH (and ethanol) electro-oxidation activity of the anode [13], taking into account that catalyst development for the cathode is focusing on enhancing the oxygen reduction activity of platinum electro-catalyst and increasing its selectivity to enhance MeOH tolerance [14].

Within such perspectives, the objective of the European project MOREPOWER [15] is to develop a low-cost, low temperature, portable DMFC, nominal power 250 W, of compact construction and modular design for the potential market area of weather stations, medical devices, signal units, gas sensors and

* Corresponding author. Tel.: +39 011 5644608; fax: +39 011 5644699.
E-mail address: stefania.specchia@polito.it (S. Specchia).

0378-7753/$ – see front matter © 2007 Elsevier B.V. All rights reserved.
doi:10.1016/j.jpowsour.2007.08.048

Nomenclature

E_a	air excess
F	Faraday constant (9.6458×10^4 C mol^{-1})
$G_{in/out/reacted}$	inlet/outlet/reacted flow in the stack (mol s^{-1})
$H_{reaction}$	reaction enthalpy (J mol^{-1})
I	current (A)
p_i	vapour pressure (bar)
p_{tot}	total pressure (bar)
P	power (W)
Q_w	waste heat (W)
T	temperature (°C)
V	voltage (V)
x_i	liquid molar fraction
y_i	vapour molar fraction
z	number of electrons

security cameras. Based on past conceptual studies and investigations of the DMFC system configuration and on modelling calculations [16,17], new scheme arrangements were proposed leading to a simple equipment architecture and a more efficient process, which entails significant economic advantages.

2. DMFC model description

The goal of system modelling is the evaluation of heat and mass fluxes and pressure drops, for the integration and optimisation of the DMFC components of a complete, lower temperature, portable Auxiliary Power Unit capable of producing electricity for portable devices of small/medium power (50–500 W). The main system components, represented in Fig. 1, are:

- the DMFC;
- the radiator (E-201) to cool the fuel solution downstream the DMFC anode;
- the gas–liquid separator (S-201, an atmospheric adiabatic flash unit) to dump up the produced CO_2 thereby limiting its presence in the anode DMFC feed;
- the catalytic burner (R-401) to burn the residual MeOH vapours before releasing the anode exhausts in the atmosphere;
- the pump (P-201) to feed the fuel solution to the DMFC anode;
- the MeOH cartridge (V-201) to feed fresh MeOH into the system;
- the water condenser (E-101) to recover and make-up the water lost during operation;
- the blower (B-101) to feed the fresh air necessary to the cathode reactions.

The addition of fresh feed solution from the MeOH cartridge (V-201) to the exhaust solution is controlled via a MeOH sensor (I-201) [18]; the controlled composition feed solution is then pumped into the DMFC, where the overall chemical reactions between the fuel and air produce power and heat. In Fig. 1 all the system sub-components used during the start-up are also represented. A small fraction of pure MeOH, taken directly from

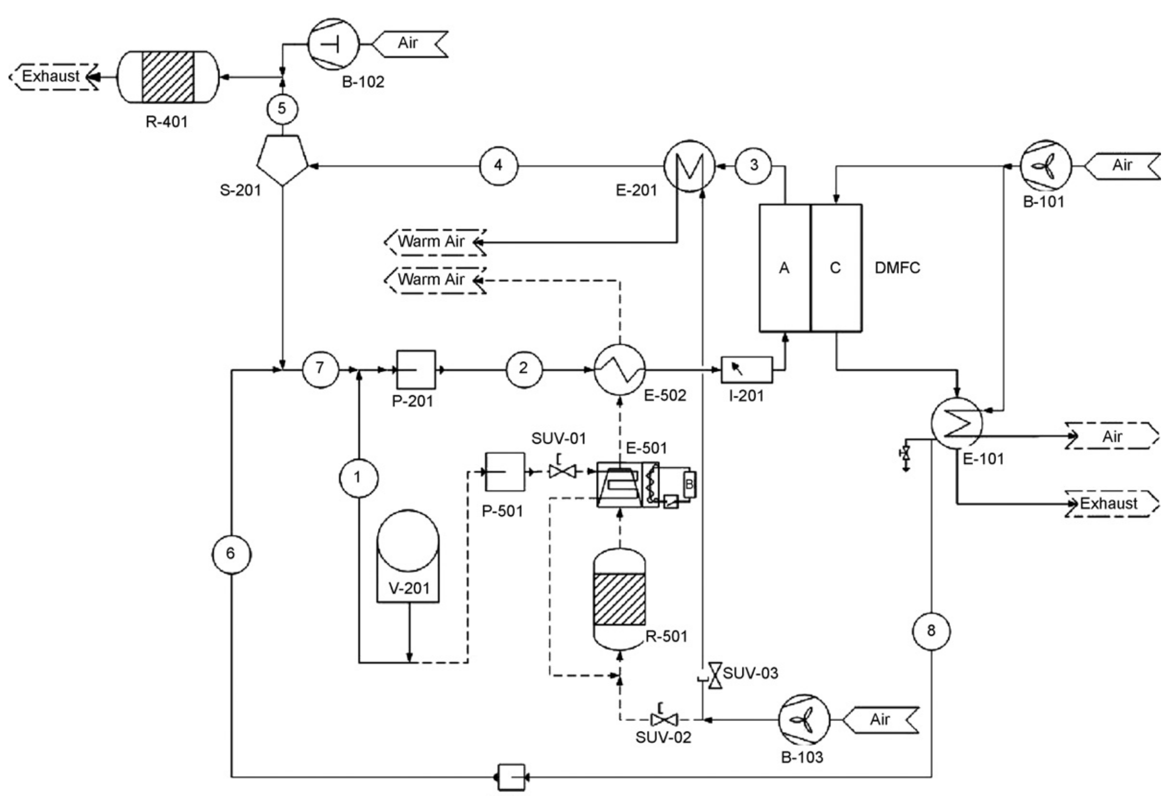

Fig. 1. MOREPOWER DMFC process scheme.

the MeOH cartridge (V-201) via a dedicated pump (P-501), is fed to an evaporator (E-501, electrically heated during the initial phase of the start-up procedure). The obtained MeOH vapour is then burned into a burner (R-501) with fresh air (B-103); the produced flue gas is used to heat-up the solution to be fed into the DMFC in the start-up heat exchanger (E-502). The direct use of MeOH in FCs is in fact considerably attractive from the point of view of system design simplicity and hence costs [19]. The nominal power demand of such a DMFC power system is 250 W, while the minimal and the maximal peak powers are 50 W and 500 W, respectively. The system was modelled with the software Matlab/Simulink®.

The DMFC system hosts the main electrochemical reactions at the anode, where MeOH is electrochemically oxidized to CO_2 according to (1), and at the cathode, where O_2 is reduced to H_2O according to (2); there is also a crossover combustion reaction at the cathode, where the permeated MeOH is oxidized according to (3). The reaction system was implemented in the software platform using the following equations:

$$CH_3OH + H_2O \rightarrow CO_2 + 6H^+ + 6e^- \quad (1)$$

$$6H^+ + (3/2)O_2 + 6e^- \rightarrow 3H_2O \quad (2)$$

$$CH_3OH + (3/2)O_2 \rightarrow CO_2 + 2H_2O \quad (3)$$

The equations for the electric current (4), the electric power (5), the overall energy balances (6 and 7) and the vapour-liquid equilibrium at the gas–liquid separator (8) were implemented into the mathematical model:

$$P = IV \quad (4)$$

$$I = zFG_{\mathrm{reacted}} \quad (5)$$

$$(G_{\mathrm{out}}H_{\mathrm{out}}) - (G_{\mathrm{in}}H_{\mathrm{in}}) + Q_{\mathrm{w}} = G_{\mathrm{reaction}}\,\Delta H_{\mathrm{reaction}} \quad \text{(balance with reaction)} \quad (6)$$

$$(G_{\mathrm{out}}H_{\mathrm{out}}) - (G_{\mathrm{in}}H_{\mathrm{in}}) + Q_{\mathrm{w}} = 0 \quad \text{(balance without reaction)} \quad (7)$$

$$p_i x_i = p_{\mathrm{tot}} y_i \quad (8)$$

The $\Delta H_{\mathrm{reaction}}$ were calculated from the heats and free energies of formation of the chemical species involved in the reactions [20]. Eq. (6) was used for the items where a chemical reaction is involved (in the stack and in the afterburner R-401), whereas Eq. (7) was employed for the ones where no chemical reaction occurs (e.g. in the radiator E-201 and in the gas–liquid separator S-201).

Two main additional aspects were taken into account in the proposed DMFC model:

- the H_2O crossover through the DMFC stack membranes, accounted for as seven times the MeOH crossover on the grounds of experimental evidences;
- the overall DMFC heat losses.

Table 1
Starting data for the simulations

Anode pressure gauge	1 bar
Cathode pressure gauge	1 bar
Ambient temperature	25 °C
Inlet temperature in the stack	60 °C
Cells number	30 or 40
Cell surface	222 cm^2 (140 cm × 140 cm)
Methanol concentration	1 M
Methanol crossover	Experimental data from C.N.R.-I.T.A.E.
Methanol excess	10 times the stoichiometric value
Water crossover	7 times methanol crossover
Air excess	2/5 times the stoichiometric value
Membrane	Type A (MORGANE CRA08) and type B (MORGANE N100-40V) by SOLVAY SA
Catalytic burner	Stoichiometric air combustion
Heat losses into the stack	$K_{\mathrm{graphite}} = 2.000\ \mathrm{W\,m^{-1}\,K^{-1}}$ (perpendicular to basal layer) and $K_{\mathrm{graphite}} = 10\ \mathrm{W\,m^{-1}\,K^{-1}}$ (parallel to basal layer)

The simulations were performed by imposing the conditions provided in Table 1, and by calculating, consequently, the sensibility of flow rates and temperatures in the eight different system streams, enlightened by the corresponding numbers in Fig. 1. All the simulations were performed at three different power level: 50–250–500 W.

Moreover, the simulations were done trying to investigate the effects on the whole system behaviour of:

- two different membrane types in the DMFC stack, given by the project partner SOLVAY SA (membrane A: type MORGANE CRA08, a radio-chemically grafted, partially fluorinated cation exchange membrane typically used in water purification applications, with reduced MeOH permeability compared to Nafion 117®; membrane B: type MORGANE N100-V40, a reduced MeOH permeability membrane variant respect to the previous one) [21]; the voltages accounted for in the model, derived from the experimental data obtained by the project partner C.N.R.-I.T.A.E.,

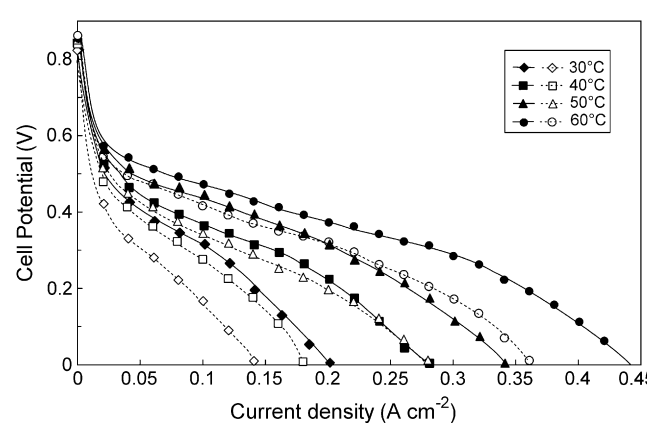

Fig. 2. Membrane type A (solid lines) and type B (dotted lines) polarization curves as a function of temperature (courtesy of C.N.R.-I.T.A.E., Messina, Italy: atmospheric pressure; MeOH = 2 ml min^{-1}, air flow = 350 ml min^{-1}).

Table 2
Experimental MeOH crossover values related to membranes type A and B implemented into the model at $T = 60\,°C$ and $p = 1$ bar (courtesy of C.N.R.-I.T.A.E., Messina, Italy)

	Membrane type A	Membrane type B
Crossover at 0.1 A cm^{-2}	5.5×10^{-6} mol min^{-1} cm^{-2}	4.2×10^{-6} mol min^{-1} cm^{-2}
Crossover at 0.2 A cm^{-2}	3.3×10^{-6} mol min^{-1} cm^{-2}	2.5×10^{-6} mol min^{-1} cm^{-2}
Crossover at 0.26 A cm^{-2}	1.6×10^{-6} mol min^{-1} cm^{-2}	1.3×10^{-6} mol min^{-1} cm^{-2}

are represented in Fig. 2, so as the crossover data are listed in Table 2;

- the number of cells composing the stack: 30 or 40 cells, respectively;
- the variation in the overall air fed at cathode side (E_a): two or five times the stoichiometric value;
- the presence of thermal insulation material over the entire stack (thermal conductivity: $K = 0.08\,W\,m^{-1}\,K^{-1}$ [20]; thickness: 1 cm).

3. Results and discussion

The main results obtained with the simulations are presented in Tables 3–5.

3.1. Simulation results of a 40 cells DMFC stack with membrane type A or B, fed with an air excess twice the stoichiometric value at three different power demands, with and without thermal insulation

By observing Table 3, the absence of thermal insulation generates an undesired effect all over the DMFC stack performance: there is in fact a slight increase of the reactant/products flow rates in every single process line. This increase reaches up to 8% at the higher power demands for both membrane types A and B. However, at lower power demands, such a phenomenon is almost imperceptible (no more than 1% increase compared to the insulated DMFC stack). Moreover, there is an evident cooling effect of the stack, especially at the lower or nominal power demands (Table 3, process lines A.3/B.3 at 50 W and 250 W and A.3 at 500 W where the reached inlet temperatures are 52.0/49.3 °C, 55.9/55.8 °C and 59.6 °C, respectively). Under these conditions the DMFC inlet flow cannot reach the operating temperature of 60 °C, except the case of 500 W, membrane type B, where the inlet temperature is approximately 61 °C (Table 3, 500 W process line B.3). As a consequence, if not properly insulated, the DMFC stack would not allow self-sustaining operation and the system would shut off. Therefore, the radiator E-201 (the heat-exchanger E-502 works only during the start-up phase) should heat up the stream instead of cooling it down. The simulation model calculations do not take these extinguishing conditions into account, but adjust the temperature of stream 3 to the fixed operative value of about 60 °C. At higher power demands (i.e. higher flow rates circulating into the stack system), this effect decreases because the MeOH consumed at the anode side increases, thus giving a larger heat production by its combustion at the cathode side, which partially compensates for the heat lost to the environment.

3.2. Simulation results of a thermally insulated 40 cells DMFC stack with membrane type A or B, fed with an air excess equal to two or five times the stoichiometric value at three different power demands

Table 4 shows that an increase in the air flow rate fed to the cathode side (E_a of five times the stoichiometric values instead of two, value normally used in the experimental practice to avoid cathode flooding) does not remarkably influence the system performance in terms of flow rates. With both membranes type A and B, the temperature of the process streams 3 decreases negligibly when E_a increases (see Table 4 process lines A.3/B.3 for 50/250/500 W and $E_a = 5$). However, another effect, more difficult to properly manage, takes place for both membranes: along with the E_a increase, the process needs an additional external make-up water at low power demands (50 W). By comparing in Table 4 the 50 W process streams A.6/B.6 (the water flow rate needed to restore the right MeOH concentration to be fed into the DMFC) with the process streams A.8/B.8 (water rate recovered at cathode outlet, usable as make-up water), one can ascertain that the former is higher than the latter. Therefore, the recovered water is not sufficient to satisfy the mass balances and achieve the steady state condition. In this specific case, an external water make-up is thus necessary. However, considering the stack performance improvement with E_a, at the expenses of the air compressor parasitic power increase, an optimisation for the E_a value could then be carried out, trying to avoid both the cathode flooding and an external water make-up.

3.3. Simulation results of a thermally insulated 40 or 30 cells DMFC stack with membrane type A or B, fed with an air excess twice the stoichiometric value at three different power demands

Table 5 shows that, for the two systems, the temperatures at the stack outlet (process stream 3) are practically the same. Conversely, for both membrane types A and B and for the three power ranges, in the case of a DMFC stack composed by 30 cells, the MeOH and H_2O rates are smaller compared to the case of 40 cells. This is due to the lower crossover values corresponding to the higher current density of the system with

Table 3
Simulation results (molar rates and *T* in the process streams) for a 40 cells DMFC stack with membrane types A or B, air excess equal to twice the stoichiometric value at three different power demands, with and without thermal insulation

Membrane and process stream	G_{MeOH} (mmol s^{-1})		G_{H_2O} (mmol s^{-1})		G_{CO_2} (mmol s^{-1})		T (°C)	
	With	Without	With	Without	With	Without	With	Without
50 W								
A.1	1.229	1.229	–	–	–	–	25.0	25.0
B.1	0.964	0.968	–	–	–	–	25.0	25.0
A.2	12.234	12.243	650.032	650.528	0.156	0.156	60.0	60.0
B.2	9.602	9.638	510.177	512.098	0.122	0.123	60.0	60.0
A.3	11.011	11.019	642.106	642.603	0.262	0.264	67.9	52.0[a]
B.3	8.642	8.674	504.080	506.002	0.226	0.231	67.6	49.3[a]
A.4	11.011	11.019	642.106	642.603	0.262	0.264	60.5	61.0
B.4	8.642	8.674	504.080	506.002	0.226	0.231	60.5	60.5
A.5	0.005	0.005	0.066	0.067	0.106	0.108	60.5	61.0
B.5	0.004	0.004	0.057	0.059	0.104	0.108	60.5	60.5
A.6	–	–	7.992	7.992	–	–	25.0	25.0
B.6	–	–	6.154	6.155	–	–	25.0	25.0
A.7	11.006	11.014	650.032	650.528	0.156	0.156	60.0	60.0
B.7	8.638	8.670	510.177	512.098	0.122	0.123	60.0	60.0
A.8	–	–	9.311	9.312	–	–	25.0	25.0
B.8	–	–	7.195	7.200	–		25.0	25.0
250 W								
A.1	1.768	1.833	–	–	–	–	25.0	25.0
B.1	1.575	1.731	–	–	–	–	25.0	25.0
A.2	17.499	18.135	929.759	963.575	0.225	0.233	60.0	60.0
B.2	15.562	17.088	826.854	907.921	0.200	0.220	60.0	60.0
A.3	15.749	16.322	922.159	956.014	0.999	1.088	68.4	55.9[a]
B.3	14.006	15.379	820.862	901.956	1.017	1.220	68.6	55.8[a]
A.4	15.749	16.322	922.159	956.014	0.999	1.088	60.4	60.4
B.4	14.006	15.379	820.862	901.956	1.017	1.220	60.4	60.4
A.5	0.018	0.020	0.251	0.273	0.775	0.856	60.4	60.3
B.5	0.018	0.022	0.255	0.306	0.817	1.000	60.3	60.3
A.6	–	–	7.852	7.835	–	–	25.0	25.0
B.6	–	–	6.247	6.270	–	–	25.0	25.0
A.7	15.731	16.302	929.759	963.575	0.225	0.233	60.0	60.0
B.7	13.987	15.357	826.854	907.921	0.200	0.220	60.0	60.0
A.8	–	–	9.892	9.962	–	–	25.0	25.0
B.8	–	–	8.092	8.322	–	–	25.0	25.0
500 W								
A.1	2.560	2.712	–	–	–	–	25.0	25.0
B.1	2.476	2.958	–	–	–	–	25.0	25.0
A.2	2.223	26.710	1340.173	1419.167	0.325	0.345	60.0	60.0
B.2	24.364	29.076	1294.517	1544.864	0.315	0.376	60.0	60.0
A.3	22.701	24.039	1333.049	1412.135	2.081	2.289	69.2	59.6[a]
B.3	21.927	26.168	1288.681	1539.113	2.185	2.810	69.6	61.1
A.4	22.701	24.039	1333.049	1412.135	2.081	2.289	60.4	60.4
B.4	21.927	26.168	1288.681	1539.113	2.185	2.810	60.4	60.4
A.5	0.038	0.041	0.520	0.572	1.755	1.944	60.3	60.3
B.5	0.039	0.050	0.545	0.700	1.870	2.434	60.2	60.2
A.6	–	–	7.644	7.604	–	–	25.0	25.0
B.6	–	–	6.381	6.452	–	–	25.0	25.0
A.7	22.663	23.998	1304.173	1419.167	0.325	0.345	60.0	60.0
B.7	21.888	26.118	1294.517	1544.864	0.315	0.376	60.0	60.0
A.8	–	–	10.743	10.907	–	–	25.0	25.0
B.8	–	–	9.417	10.127	–	–	25.0	25.0

[a] Extinguishing conditions.

30 cells, the power being the same. The higher current density is also responsible for the anodic produced CO_2, which increases for the stack with 30 cells compared to the 40 cells one. As a consequence, the same occurs for the CO_2 rate at the gas–liquid separator (Fig. 1, S-201); such a rate is higher for the 30 cells stack than for the 40 cells one, and it increases with the system power (see Table 5, process streams A.5/B.5 30/40 cells, at any power range). The obtained results are very

Table 4
Simulation results (molar rates and T in the process streams) for a thermally insulated 40 cells DMFC stack with membrane types A or B, air excess equal to two or five times the stoichiometric value at three different power demands

Membrane and process stream	G_{MeOH} (mmol s^{-1})		G_{H_2O} (mmol s^{-1})		G_{CO_2} (mmol s^{-1})		T (°C)	
	$E_a=2$	$E_a=5$	$E_a=2$	$E_a=5$	$E_a=2$	$E_a=5$	$E_a=2$	$E_a=5$
50 W								
A.1	1.228	1.228	–	–	–	–	25.0	25.0
B.1	0.964	0.964	–	–	–		25.0	25.0
A.2	12.234	12.234	650.032	650.038	0.156	0.156	60.0	60.0
B.2	9.602	9.602	510.177	510.198	0.122	0.122	60.0	60.0
A.3	11.011	11.011	642.106	642.113	0.262	0.262	67.9	67.7
B.3	8.642	8.642	504.080	504.101	0.226	0.227	67.6	67.4
A.4	11.011	11.011	642.106	642.113	0.262	0.262	60.5	60.5
B.4	8.642	8.642	504.080	504.101	0.226	0.227	60.5	60.5
A.5	0.005	0.005	0.066	0.066	0.106	0.106	60.5	60.5
B.5	0.004	0.004	0.057	0.057	0.104	0.104	60.5	60.5
A.6	–	–	7.992	7.992	–	–	25.0	25.0
B.6	–	–	6.154	6.154	–	–	25.0	25.0
A.7	11.006	11.006	650.032	650.038	0.156	0.156	60.0	60.0
B.7	8.638	8.638	510.177	510.198	0.122	0.122	60.0	60.0
A.8	–	–	9.311	7.685	–	–	25.0	25.0
B.8	–	–	7.195	5.933	–	–	25.0	25.0
250 W								
A.1	1.768	1.769	–	–	–	–	25.0	25.0
B.1	1.575	1.576	–	–	–	–	25.0	25.0
A.2	17.499	17.508	929.759	903.233	0.225	0.225	60.0	60.0
B.2	15.562	15.579	826.854	827.729	0.200	0.200	60.0	60.0
A.3	15.749	15.757	922.159	922.634	0.999	1.001	68.4	68.3
B.3	14.006	14.021	820.862	821.738	1.017	1.019	68.6	68.4
A.4	15.749	15.757	922.159	922.634	0.999	1.001	60.4	60.4
B.4	14.006	14.021	820.862	821.738	1.017	1.019	60.4	60.4
A.5	0.018	0.018	0.251	0.251	0.775	0.776	60.4	60.4
B.5	0.018	0.018	0.255	2.256	0.817	0.819	60.3	60.3
A.6	–	–	7.852	7.852	–	–	25.0	25.0
B.6	–	–	6.247	6.247	–	–	25.0	25.0
A.7	15.731	15.739	929.759	903.233	0.225	0.225	60.0	60.0
B.7	13.987	14.003	826.854	827.729	0.200	0.200	60.0	60.0
A.8	–	–	9.892	7.999	–	–	25.0	25.0
B.8	–	–	8.092	6.499	–	–	25.0	25.0
500 W								
A.1	2.560	2.562	–	–	–	–	25.0	25.0
B.1	2.476	2.482	–	–	–	–	25.0	25.0
A.2	25.223	25.246	1340.173	1341.377	0.325	0.326	60.0	60.0
B.2	24.364	24.421	1294.517	1297.554	0.315	0.316	60.0	60.0
A.3	22.701	22.721	1333.049	1334.254	2.081	2.084	69.2	69.1
B.3	21.927	21.979	1288.681	1291.719	2.185	2.192	69.6	69.5
A.4	22.701	22.721	1333.049	1334.254	2.081	2.084	60.4	60.4
B.4	21.927	21.979	1288.681	1291.719	2.185	2.192	60.4	60.4
A.5	0.038	0.038	0.520	0.521	1.755	1.758	60.3	60.3
B.5	0.039	0.039	0.545	0.547	1.870	1.877	60.2	60.2
A.6	–	–	7.644	7.644	–	–	25.0	25.0
B.6	–	–	6.381	6.381	–	–	25.0	25.0
A.7	22.663	22.684	1304.173	1341.377	0.325	0.326	60.0	60.0
B.7	21.888	21.393	1294.517	1297.554	0.315	0.316	60.0	60.0
A.8	–	–	10.743	8.459	–	–	25.0	25.0
B.8	–	–	9.417	7.336	–	–	25.0	25.0

interesting: it is indeed possible to work with reduced MeOH rate and with a most compact system using only 30 cells DMFC stack. These considerations are valid for both membrane types A and B, but in case of membrane B the reactant flow rates are smaller (i.e., membrane type B seems to behave more efficiently). Such a difference, especially related to the fresh MeOH to be fed to the system, decreases when the power demand is increased.

Table 5
Simulation results (molar rates and T in the process streams) for a thermally insulated 40 or 30 cells DMFC stack with membrane types A or B, air excess equal to twice the stoichiometric value at three different power demands

Membrane and process stream	G_{MeOH} (mmol s^{-1})		G_{H_2O} (mmol s^{-1})		G_{CO_2} (mmol s^{-1})		T (°C)	
	40 cells	30 cells	40 cells	30 cells	40 cells	30 cells	40 cells	30 cells
50 W								
A.1	1.228	0.944	–	–	–	–	25.0	25.0
B.1	0.964	0.748	–	–	–	–	25.0	25.0
A.2	12.234	9.401	650.032	499.496	0.156	0.120	60.0	60.0
B.2	9.602	7.438	510.177	395.218	0.122	0.095	60.0	60.0
A.3	11.011	8.461	642.106	493.566	0.262	0.228	67.9	67.6
B.3	8.642	6.694	504.080	390.650	0.226	0.201	67.6	67.2
A.4	11.011	0.004	642.106	493.566	0.262	0.228	60.5	60.5
B.4	8.642	0.004	504.080	390.650	0.226	0.201	60.5	60.5
A.5	0.005	–	0.066	0.058	0.106	0.108	60.5	60.5
B.5	0.004	–	0.057	0.051	0.104	0.106	25.0	60.5
A.6	–	–	7.992	5.988	–	–	25.0	25.0
B.6	–	–	6.154	4.619	–	–	25.0	25.0
A.7	11.006	8.457	650.032	499.496	0.156	0.120	60.0	60.0
B.7	8.638	6.690	510.177	395.218	0.122	0.093	60.0	60.0
A.8	–	–	9.311	7.008	–	–	25.0	25.0
B.8	–	–	7.195	5.432	–	–	25.0	25.0
250 W								
A.1	1.768	1.508	–	–	–	–	25.0	25.0
B.1	1.575	1.390	–	–	–	–	25.0	25.0
A.2	17.499	14.898	929.759	791.555	0.225	0.192	60.0	60.0
B.2	15.562	13.715	826.854	728.713	0.200	0.177	60.0	60.0
A.3	15.749	13.408	922.159	785.963	0.999	0.998	68.4	68.5
B.3	14.006	12.343	820.862	724.256	1.017	1.034	68.6	68.7
A.4	15.749	13.408	922.159	785.963	0.999	0.998	60.4	60.4
B.4	14.006	12.343	820.862	724.256	1.017	1.034	60.4	60.4
A.5	0.018	0.018	0.251	0.250	0.775	0.806	60.4	60.3
B.5	0.018	0.019	0.255	0.259	0.817	0.857	60.3	60.3
A.6	–	–	7.852	5.841	–	–	25.0	25.0
B.6	–	–	6.247	4.716	–	–	25.0	25.0
A.7	15.731	13.390	929.759	791.555	0.225	0.192	60.0	60.0
B.7	13.987	12.325	826.854	728.713	0.200	0.177	60.0	60.0
A.8	–	–	9.892	7.641	–	–	25.0	25.0
B.8	–	–	8.092	6.377	–	–	25.0	25.0
500 W								
A.1	2.560	2.409	–	–	–	–	25.0	25.0
B.1	2.476	2.338	–	–	–	–	25.0	25.0
A.2	25.223	23.693	1340.173	1258.860	0.325	0.306	60.0	60.0
B.2	24.364	22.975	1294.517	1200.703	0.315	0.297	60.0	60.0
A.3	22.701	21.324	1333.049	1253.811	2.081	2.229	69.2	69.8
B.3	21.927	20.677	1288.681	1216.410	2.185	2.262	69.6	70.0
A.4	22.701	21.324	1333.049	1253.811	2.081	2.229	60.4	60.4
B.4	21.927	20.667	1288.681	1216.410	2.185	2.262	60.4	60.3
A.5	0.038	0.040	0.520	0.556	1.755	1.923	60.3	60.2
B.5	0.039	0.041	0.545	0.564	1.870	1.956	60.2	60.2
A.6	–	–	7.644	5.605	–	–	25.0	25.0
B.6	–	–	6.381	4.857	–	–	25.0	25.0
A.7	22.663	21.284	1304.173	1258.860	0.325	0.306	60.0	60.0
B.7	21.888	20.637	1294.517	1220.703	0.315	0.297	60.0	60.0
A.8	–	–	10.743	8.584	–	–	25.0	25.0
B.8	–	–	9.417	7.771	–	–	25.0	25.0

4. Conclusions

A conceptual study of a 250 W nominal power DMFC system was carried out in Matlab/Simulink® platform: the scheme arrangement proposed lead to a simple equipment architecture and a more efficient process, based on the following obtained results:

(i) The DMFC system can be operated, with both membrane types A or B, in an self-sustaining way only if properly insulated; if the DMFC is not insulated, the stack with membrane type A is not thermally self-sustaining (the system is an extinguishing one), unless the stack anode feed flow is heated at all power ranges.

(ii) With the DMFC system working with a five times higher than stoichiometric air excess at the cathode side, independently of the membrane type, insufficient make-up water is recovered from the stack; thus an external water make-up is necessary. This problem is avoided if the DMFC system works with twice the stoichiometric air excess at the cathode side.

(iii) The DMFC system can be operated with 30 o 40 cells independently of the membrane type employed. The advantage of a 30 cells DMFC stack is, of course, its higher compactness.

(iv) In all the considered cases, with membrane type B, notwithstanding its lower conductivity, the system consumes less reactants than the one working with membrane type A; membrane B entails a more efficient system operation. This is also due to the lower MeOH crossover values characterising this type of membrane.

Therefore, a DMFC composed by a properly insulated 30 cells stack, membrane type B fed with an air excess only twice the stoichiometric value should guarantee an autonomous operation of portable devices, with high compactness and low fuel consumption.

Acknowledgments

The authors gratefully acknowledge the financial support of the European Commission for the MOREPOWER project (compact direct methanol fuel cells for portable applications, project nr. SES6-CT-2003-502652) and all the involved partners: GKSS Forschungszentrum (D), Centro Ricerche Fiat (I), SOLVAY SA (B), Johnson Matthey (UK), Consiglio Nazionale delle Ricerche—Istituto di Tecnologie Avanzate per l'Energia "Nicola Giordano" (I), Institut für Mikrotechnik Mainz (D), Nedstack Fuel Cell Technology & Components (NL).

References

[1] Kyoto Protocol to the United Nations Framework Convention on Climate Change, English Conference of the Parties, Third Session, Kyoto (1997).
[2] R. Dillon, S. Srinivasan, A.S. Aricò, V. Antonucci, J. Power Sources 127 (2004) 112–126.
[3] A. Heinzel, V.M. Barragan, J. Power Sources 84 (1999) 70–74.
[4] D.H. Jung, C.H. Lee, C.S. Kim, D.R. Shin, J. Power Sources 71 (1998) 169–173.
[5] P. Costamagna, S. Srinivasan, J. Power Sources 102 (2001) 242–252.
[6] A. Oedegaard, J. Power Sources 157 (2006) 244–252.
[7] A.S. Aricò, V. Baglio, E. Modica, A. Di Blasi, V. Antonucci, Electrochem. Commun. 6 (2004) 164–169.
[8] G. Cacciola, V. Antonucci, S. Freni, J. Power Sources 100 (2001) 67–79.
[9] S. Banerjee, D.E. Curtin, J. Fluor. Chem. 125 (2004) 1211–1216.
[10] Y.Z. Fu, A. Manthiram, J. Power Sources 157 (2006) 222–225.
[11] V.S. Silva, A. Mendesa, L.M. Madeira, S.P. Nunes, J. Membr. Sci. 276 (2006) 126–134.
[12] D.S. Kim, K.H. Shin, H.B. Park, Y.S. Chung, S.Y. Nam, Y.M. Lee, J. Membr. Sci. 278 (2006) 428–436.
[13] A. Oliveira Neto, E.G. Franco, E. Aricò, M. Linardi, E.R. Gonzales, J. Eur. Ceram. Soc. 23 (2003) 29872992.
[14] V. Baglio, A.S. Aricò, A. Di Blasi, V. Antonucci, P.L. Antonucci, S. Licoccia, E. Traversa, Electrochim. Acta 50 (2005) 1241–1246.
[15] EU funded project MOREPOWER (compact direct methanol fuel cells for portable applications), project nr. SES6-CT-2003-502652 (2004).
[16] S. Specchia, U.A. Icardi, V. Specchia, G. Saracco, Int. J. Chem. React. Eng. 3 (2005) A24.
[17] S.S. Sandhu, R.O. Crowther, J.P. Fellner, Electrochim. Acta 50 (2005) 3985–3991.
[18] M. Sgroi, G. Bollito, G. Innocenti, G. Saracco, S. Specchia, U.A. Icardi, J. Fuel Cell Sci. Technol. 4 (2007) 345–349.
[19] A.K. Shukla, C.L. Jackson, K. Scott, G. Murgia, J. Power Sources 111 (2002) 43–51.
[20] R.H. Perry, D.W. Green, Perry's Chemical Engineer's Handbook, 7th ed., McGraw-Hill International Editions, 1997.
[21] V. Antonucci, A.S. Aricò, V. Baglio, J. Brunea, I. Buder, N. Cabello, M. Hogarth, R. Martin, S. Nunes, Desalination 200 (2006) 653–655.